Stacking dependent disordering processes in Gd/Co/Pt(111) studied with surface x-ray diffraction

C. Quirós,[1,*] I. Popa,[2,†] O. Robach,[3] D. Wermeille,[2] J. Díaz,[1] R. Felici,[2] and S. Ferrer[4]
[1]*Departamento de Física, Universidad de Oviedo-CINN, Avenida Calvo Sotelo s/n, 33007 Oviedo, Spain*
[2]*European Synchrotron Radiation Facility, BP 220, 38043 Grenoble Cedex, France*
[3]*CEA-Grenoble INAC/SP2M/NRS, 17 rue des Martyrs, 38054 Grenoble Cedex 9, France*
[4]*ALBA, apartado de correos 68, 08193 Bellaterra, Spain*
(Received 13 June 2008; revised manuscript received 16 September 2008; published 6 November 2008)

Disordering processes induced by Gd overlayers on 15 atomic layers thick Co films grown on top of a Pt(111) surface have been studied *in situ* by surface x-ray diffraction. They have been investigated in two structurally different Co layers deposited at different substrate temperatures: a film grown at 220 K consisting of a mixture of hcp and fcc crystallites plus some disordered stacking, and another one grown at room temperature containing more disorder and fcc crystallites only. Gd induced disordering has been found to be dependent on the structure of the Co film since cubic fcc crystallites are more sensitive to disordering than hexagonal ones. In addition, Gd deposition causes a reduction in about 0.5% in the Co interatomic distance in the layer plane, which arises from relaxation of stress in the film. The stress is mainly concentrated in fcc grains, which are more strained in the film plane than hcp ones. Furthermore, Co grains having the substrate fcc stacking sequence are majority in the Co films, and they are more stable against disordering than the corresponding fcc twin ones, suggesting some kind of long-range interaction stabilizing the majority stacking. These structural modifications induced by the Gd overlayers affect the magnetism of the film, as evidenced by the hysteresis loops measured by magneto-optical Kerr effect, probing the Co magnetization, and by resonant x-ray scattering at the Pt L_{III} edge, sensitive to the Pt magnetization at the Co/Pt interface. It has been found that the Gd overlayer changes the magnetization of the whole Co film, increasing significantly its coercive field for thick enough Gd overlayers and reducing the amplitude of the loops. These changes are compatible with the formation of a disordered Co-Gd alloy with reduced magnetic moment for the Co atoms, and they affect the whole Co film down to the Pt interface. All these results illustrate how surface x-ray diffraction can be used to characterize in detail alloying processes happening in thin films of binary systems, especially in those containing heterogeneous mixtures of different phases.

DOI: 10.1103/PhysRevB.78.195406 PACS number(s): 68.55.−a, 68.35.−p, 75.70.−i

I. INTRODUCTION

Rare earth–transition metal (RE-TM) multilayers and alloys have been intensively studied since they present a rich variety of magnetic configurations that are interesting from both fundamental and applied points of view. In particular, the antiferromagnetic coupling between the magnetic moments of RE and TM atoms leads to peculiar situations when the net magnetization of RE and TM sublattices are similar. The temperature at which this situation takes place is called compensation temperature and is dependent on composition.[1] In the vicinity of this temperature, magnetic thermal hysteresis can be observed[2] and the coercive field strongly diverges. The combination of this marked temperature dependence of the coercive field and the possibility of tailoring strong perpendicular anisotropies[3–5] makes this kind of systems very well suited for thermally assisted magneto-optic recording applications.

Belonging to this group of materials, $Gd_{1-x}Co_x$ alloys and multilayers show a strong trend to develop solid-state reactions (SSR) and diffusion processes leading to amorphization.[6–8] This trend is consistent with the negative heat of mixing of the system and the difference in atomic size between Co and Gd atoms (Co atomic radius/Gd atomic radius ~0.35). Transmission electron microscopy (TEM) and grazing incidence x-ray diffraction (GIXR) indicate that the amorphization is not symmetric, being more pronounced when Co is grown on top of Gd than when Gd is deposited on top of Co.[7] These SSR complicate the fabrication of Co/Gd multilayers, leading to modifications of their nominal structure. In fact, thinned Co layers[9,10] and Gd-Co amorphous alloys with composition close to the eutectic point, $Gd_{63}Co_{37}$,[11] have to be included at the Gd/Co interfaces in order to simulate the structure and temperature dependence of the magnetization of Co/Gd multilayers.[12,13] It is also known that amorphization does not proceed indefinitely at room temperature (RT), but stops when the interface reaches a composition in the range $x=0.4-0.6$. This has been used to prepare $Gd_{1-x}Co_x$/Co multilayers with lower Co thickness, even down to just 6 Å.[14,15] In fact, multilayers based on exchange-coupled amorphous Gd-Co alloys have been successfully prepared with peculiar configurations of the magnetization.[16] All these results have allowed developing a semiempirical thermodynamical model of the Co-Gd reaction which predicts stable compositions of the amorphous alloys formed in Co/Gd multilayers in good agreement with the experimental values.[17] However, the microscopic details on how the amorphization takes place are poorly known and new data are needed in order to improve the comprehension of this kind of processes. Apart from this fundamental motivation, increasing understanding on the disordering phenomena might be of practical interest, since magnetic properties such as coercivity, anisotropy, and exchange coupling in binary alloys of amorphous systems strongly differ from those of the crystallized material.[18,19]

Furthermore, there are many amorphous binary alloys based on Co, not only with Gd or other RE, but with elements such as Zr, Ti, Si, P, or B,[20–24] among many others, which are relevant both for their properties and applications. Gaining insight on the way in which Co crystals disorder as they mix with other elements may be useful to improve the understanding of the relation between structure and properties in these Co based alloys. Especially important for this improvement is to characterize in detail how the different stackings usually observed in Co films (fcc, hcp, or disordered sequences) mix with other elements to form disordered alloys. In this way, a fine tuning of their properties can be achieved by controlling the Co stacking distribution before disordering by overlayers takes place.

In relation to this, one simple strategy to control the hcp/fcc balance in Co films consists of selecting adequate substrates and growth temperatures. In particular, Pt(111) substrates are specially well suited to tune the structure of Co films since they grow following the substrate in-plane symmetry, but the out-of-plane atomic arrangement strongly depends on the substrate temperature during growth.[25,26] Whereas growth at 120 K leads to predominantly hcp Co films with low roughness, Co films grown at room temperature exhibit fcc stacking with a large proportion of disorder, a high concentration of stacking faults and rougher surfaces. These structural and morphological properties strongly affect the magnetism of the films. Co films grown at room temperature show an abrupt transition at six monolayers thickness, since thinner films have perpendicular magnetic anisotropy whereas for thicker films the magnetic easy axis is in the film plane. On the other hand, Co films grown at low temperature do not show an abrupt spin reorientation transition, but the magnetization slowly evolves from perpendicular to parallel through intermediate canted states. In contrast with films prepared at room temperature, films of 20 atomic layers (AL) grown at 120 K have a magnetization with a significant out-of-plane component, the reason being the high proportion of hcp Co in the low-temperature films with the *c* axis along the film normal, which strongly contributes to perpendicular magnetization.[26]

This possibility of tuning the Co stacking from mainly hcp to mainly fcc simply by adjusting the Pt(111) substrate temperature during growth makes the Co/Pt(111) system very interesting to study the sensitivity of different stackings to disordering by overlayers. As it will be illustrated below, it has been found with surface x-ray diffraction that fcc stacking is more strained and more easily disordered by Gd overlayers than hcp stacking. This result will be discussed in detail, as well as the associated changes in the structure and magnetization. All this information may contribute to a better understanding of interface phenomena in which disordering and diffusion play a significant role and may stimulate new theoretical approaches to improve the modeling of the SSR observed, not only in Co-Gd or other Co based alloys but in many similar binary systems.

The paper is organized as follows: Sec. II shows the experimental details; Sec. III A presents and discusses the structural results concerning the disordering of 15 AL thick Co films by Gd overlayers, whereas in Sec. III B the corresponding magnetic properties are shown and discussed; finally, Sec. IV summarizes the main conclusions.

II. EXPERIMENTAL

The experiments were carried out in the UHV chamber (10^{-10} mbar base pressure) mounted on the six-circle diffractometer of the ID03 surface diffraction beamline at the European Synchrotron Radiation Facility (ESRF).[27] A Pt(111) substrate was used (disk shaped, 1.5 mm thick). The sample holder allowed to anneal the sample up to ~1300 K and to cool it down to ~200 K. An ion gun was used to prepare the Pt(111) surface by sputtering (2 keV Ar^+ ions) and annealing (1250 K) cycles combined with O_2 treatments to remove residual C. The Co/Gd films were deposited from two water-cooled electron bombardment evaporators. Deposition rates were in the order of 6 min/1 AL of Co and 22 min/1 AL of Gd, where 1 AL Co stands for 2.08 Å thickness, whereas 1 AL Gd is equivalent to 2.89 Å. The substrate was maintained at room temperature or at low temperature (LT) (200–220 K) during deposition.

The structural characterization was carried out by surface x-ray diffraction (SXRD) using photons in the vicinity of the Pt L_{III} atomic absorption edge (which is at 11.564 keV) at a fixed incident angle of 1° (except for the specular scans). An hexagonal reference system $\{\boldsymbol{A}_1,\boldsymbol{A}_2,\boldsymbol{A}_3\}$, based on the Pt(111) substrate lattice, was used for the whole experiment. Vectors $\boldsymbol{A}_1$ and $\boldsymbol{A}_2$ lie in the surface plane and have a modulus equal to the nearest-neighbor distance, $a_0/\sqrt{2}$, whereas vector $\boldsymbol{A}_3$ is perpendicular to the surface and has a modulus of $\sqrt{3}a_0$, with the Pt lattice constant $a_0=3.92$ Å. Accordingly, the corresponding reciprocal-lattice axes *H* and *K* are in the surface plane, whereas *L* is pointing perpendicular to the surface, following the usual convention in surface x-ray diffraction. The substrate was mounted in horizontal geometry with its surface normal in the horizontal plane.

The magnetic characterization was performed by combining magneto-optical Kerr effect (MOKE) hysteresis loops, sensitive to Co magnetization, and resonant magnetic surface x-ray diffraction (RM-SXRD) hysteresis cycles, probing the Pt magnetization at the Co/Pt interface. The MOKE setup has been described elsewhere.[26] As a result of the MOKE geometry used, the detected signal is sensitive to both transverse and polar components of the Co magnetization. It should be pointed out that when the polar component is present, it largely dominates the loop and high coercive fields are obtained.[26] The magnetic fields are generated by magnetized iron yokes inside the vacuum chamber. The maximum field intensities at the sample are around 1400 Oe for the in-plane component and around 200 Oe for the out-of-plane one.

RM-SXRD loops have been measured in transverse geometry (magnetic field applied in the substrate surface plane and perpendicular to the incoming photon beam) by taking advantage of the resonant effects appearing when the photon wavelength is tuned to the Pt L_{III} absorption line due to magnetization dependent electronic transitions between $2p$ and $5d$ Pt states. In the resonant case, following the formalism developed by de Bergevin *et al.*[28] adapted for the experimental geometry used in this experiment (linearly polarized in-

coming photons at grazing incidence and magnetization in the vertical direction), the scattering amplitude for Pt atoms, f^{Pt}, can be written, in electron radius r_0 units, as:[29]

$$f^{\mathrm{Pt}} = \cos\ \gamma(f_0 + f' - if'') + a_{\mathrm{res}}, \quad (1)$$

where f_0 is the usual Thomson charge scattering term, and f' and f'' are the anomalous contributions from dispersive and absorptive processes to the scattering amplitude, γ is the exit angle of the photons with respect to the film plane, and a_{res} is the resonant term containing the magnetization dependence. This term can be expressed as

$$a_{\mathrm{res}} = (i + x)(-n_p \cos\ \gamma - i\varepsilon n_m \sin\ \gamma \cos\ \delta)/(1 + x^2), \quad (2)$$

where n_p refers to the white line at the absorption edge (4.3 according to de Bergevin *et al.*[28]), ε is 1 or −1 depending on the up or down orientation of the magnetization, x is the relative photon energy deviation from the resonance, and δ is the in-plane angle given by the projection of the incoming and outgoing photons. The dependence to magnetization in this resonant term, keeping just first-order contributions, appears in the factor $n_m = [F_1^1 - F_{-1}^1]$, which is the difference in the transition probability of dipolar transitions involving changes in angular momentum Δj_z of 1 and −1. When the conduction band is split due to the exchange interaction, n_m is nonzero, and can be seen, roughly, as being proportional to the magnetic moment of the Pt atoms.[29] This dependence of f^{Pt} with the Pt magnetization leads to small changes in the diffracted intensity when the magnetic moments of Pt change, and it can be used to acquire Pt specific hysteresis loops. In order to do so, a well suited location in the reciprocal space has to be chosen so that the geometrical terms included in Eqs. (1) and (2) maximize the magnetic resonant contribution. In the particular case of Co/Pt(111), using grazing incidence incoming photons with linear polarization in the horizontal plane, these contributions are high at places around (0 1 3.6), or in-plane equivalents such as (1 −1 3.6), which enhance interface sensitivity, being close to the minimum of a crystal truncation rod, and have a high out-of-plane exit angle.[25] Finally, the criteria followed to make the fine tuning of the photon energy, with around 1 eV accuracy, was the maximization of the amplitude of the Pt resonant magnetic hysteresis loop, leading to the final value of 11.561 keV, which was used for all the measurements shown in this work.

It is important to keep in mind the differences between both MOKE and RM-SXRD. MOKE loops are basically sensitive to Co magnetization (since magneto-optical constants of Gd and Pt are negligible when compared to Co ones), whereas RM-SXRD loops measure the magnetization of the Pt atoms at the Co/Pt interface.[25] This means that changes in the magnetization of the Co film affecting the interface can be detected with the RM-SXRD loops. Also, due to the horizontal polarization of the incoming x-ray beam and the geometrical dependencies included in Eqs. (1) and (2), RM-SXRD loops are sensitive only to the transverse component of the Pt magnetization, in contrast with MOKE, which is sensitive to transverse and polar components.

Finally, it should be remarked that all the structural and magnetic characterizations were carried out at LT (200–220 K) in the same UHV chamber, without exposing the films to air, so that the use of capping layers could be avoided, and the direct relationship between structural and magnetic measurements could be established without introducing a new interface (capping layer/sample) that might have some additional undesired effects.

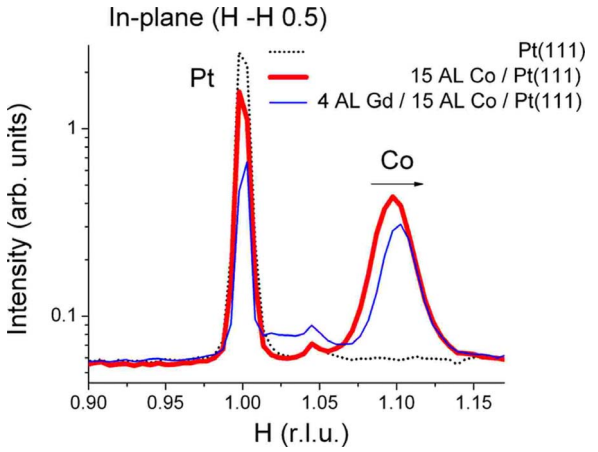

FIG. 1. (Color online) In-plane (H $-H$ 0.5) radial scans of clean Pt(111) (dotted line), 15 AL Co/Pt(111) (thick continuous line) and 4 AL Gd/15 AL Co/Pt(111) (thin line), prepared at LT. The arrow indicates the shift of the Co peak after depositing the Gd film.

III. RESULTS AND DISCUSSION

A. Structural characterization

In this section, the modifications induced by Gd overlayers on the structure of 15 AL thick Co films grown on top of the Pt substrate are presented and discussed. To this purpose, the evolution of in-plane (H $-H$ 0.5) radial scans, containing information on in-plane film ordering and of out-of-plane (1.1 −1.1 L) scans, sensitive to the Co stacking sequence, has been investigated as Gd is deposited on top.

Initially, 15 AL of Co were deposited on a clean Pt(111) surface that was kept at around 220 K. The growth was monitored by measuring the diffracted intensity at the (0 0 1.44) location in reciprocal space, close to a minimum of the Pt specular curve, which has maxima at L=0,3,6… reciprocal-lattice units (rlu). In this position, the intensity is extremely sensitive to changes in the sample morphology and roughness. The signal oscillated, with a small damping, during the whole growth sequence, indicating a close to layer-by-layer growth and a low roughness film. The good quality of the low-temperature growth, as compared to RT grown films, is a typical behavior of Co films deposited on Pt(111),[26] most likely related to the irregular shape of the Co islands observed at LT, with high density of kinks and concave corners,[30] which may favor mass transport to lower layers, as compared to RT islands with straight steps.

As already mentioned, the in-plane structure of the LT Co film has been studied by measuring radial (H $-H$ 0.5) scans, crossing the (1 −1 0.5) Pt substrate reflection. Figure 1 shows this scan for the clean Pt substrate (dotted line), having just one intense peak at H=1, corresponding to the sub-

strate periodicity. A second peak appears after growth of the Co film at $H=-K=1.10$ (thick line). This separated new reflection is indicating that Co has grown with its own in-plane lattice spacing (10% shorter than that of Pt). The figure also shows the same radial scan obtained after depositing 4 AL of Gd on top of the Co film (thin line). Aside from the expected intensity reduction in the Pt and Co reflections due to absorption effects, a very interesting result is evident from the figure: the position of the Co reflection shifts by 0.4%, which indicates that the in-plane Co-Co distance decreases by 0.4% due to the Gd deposition. This behavior will be further discussed later. No reflections attributable to Gd in-plane ordering were observed at this coverage.

Further growth of Gd up to 15 AL leads to the formation of a broad new peak at around 0.8 rlu (not shown) which was not observed at 4 AL Gd coverage. Azimuthal scans around this broad peak did not show any structure. Additional radial $(H\ -H\ L)$ scans measured at higher values of L confirmed a typical diffraction ringlike behavior, with lateral shifts in the H value of the peak, but keeping constant the 2θ value of the reflection. The large width in reciprocal space plus the structureless azimuthal scan are indicative of a high degree of disorder and small grain size in the Gd film grown on top of Co, in good agreement with previous findings.[6] The position of the radial broad feature corresponds in direct space to 3.5 Å, which is close to the expected Gd-Gd in-plane distance of 3.6 Å. No additional shift of the Co reflection occurs after thickening the Gd film from 4 to 15 AL.

The out-of-plane structure of the Co film has been studied by acquiring L scans at in-plane coordinates corresponding to the Co in-plane periodicity, which, as observed in Fig. 1, are: $H=-K=1.1$. The main interest of this $(1.1\ -1.1\ L)$ scan is that it is sensitive to the different stacking sequences that Co films may follow, since it has peaks at different L values for each of them. In more details, Co films usually exhibit three types of stacking sequences. Two of them are consequence of second-neighbor interplanar interactions, leading to *ABCABCABC*… fcc stackings (and the corresponding twin *ACBACBACB*…) or to *ABABAB*… hcp stackings. The third alternative stacking arrangement corresponds to a disordered sequence in which there is only a nearest-neighbor interplanar correlation (and not second-neighbor-like needed for fcc or hcp) that forces each plane to be different from the previous and next ones with no constrain on the second-neighbor planes. In this case, if first layer is A, the probability of having again A in the second layer is 0%, whereas the probability of having B is 50%, and of having C is also 50%. For the third plane, the probability of having A again is 50%, and so on. If the probability of having B or C in the $(m-1)$th plane (being $m=0$ the first A layer) is $1-P_{m-1}$, then the probability that the mth plane is A again can be written as $P_m=(1-P_{m-1})/2$. This can be expressed as $P_m=1/3+(2/3)\ (-1/2)^{|m|}$, and, when m is large, makes P_m tend to 1/3.[31] The type of stacking sequence that is obtained in this way is something like *ABACBACBCACACB*… As already mentioned, these three stackings give rise to different peaks at different L values in the $(1.1\ -1.1\ L)$ scan. The fcc sequence leads to a peak at $L=2\times1.1=2.2$ (1.1 times the Pt substrate fcc sequence, that has a peak at $L=2$) or at $L=1.1$ for the twin fcc stacking. For hcp stacking, three peaks are predicted at $L=0$, $L=1.5\times1.1=1.65$ and at $L=3\times1.1=3.3$. The disordered stacking leads to a unique and broader peak at $L=1.5\times1.1=1.65$. The intensities and widths of these contributions can be calculated by using a model by Guinier[31] that evaluates the intensity diffracted by a set of N planes, characterized by an interplanar correlation function, as a Fourier series of $2N$ terms where the coefficients correspond to the magnitude of the correlations between planes situated at different distances, and the result is shown in Fig. 2(a).

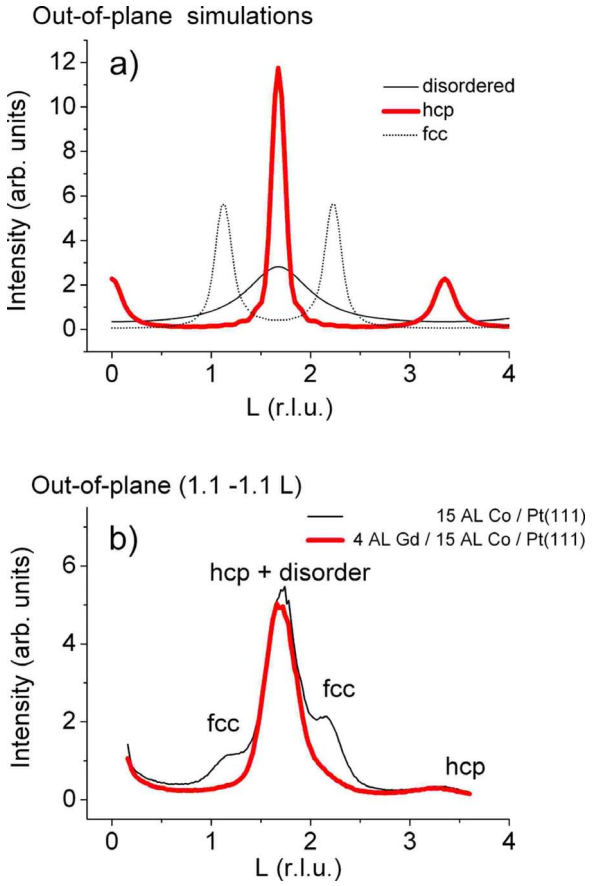

FIG. 2. (Color online) (a) Out-of-plane $(1.1\ -1.1\ L)$ calculation for the three possible stackings of Co films: fcc, hcp, or disordered. (b) Experimental out-of-plane $(1.1\ -1.1\ L)$ scans for the 15 AL Co/Pt(111) structure grown at LT before (thin line) and after (thick line) adding a 4 AL Gd overlayer.

In Fig. 2(b) measurements corresponding to this $(1.1\ -1.1\ L)$ scan are shown before (thin line) and after (thick line) growing a 4 AL Gd overlayer on top of the 15 AL Co LT film. The qualitative comparison between the calculations shown on Fig. 2(a) and the experimental data from Fig. 2(b) lead to several important conclusions. First, the 15 AL Co LT film has grown with a mixture of hcp (maybe with a small disordered contribution), as confirmed by the presence of two peaks at $L=1.65$ and 3.3, and also of both fcc stackings, as indicated by the shoulders at $L=1.1$ and 2.2. Interestingly, the peak at $L=2.2$ is more intense than the one at $L=1.1$, indicating that the Pt majority stacking [that has a peak at $(1\ -1\ 2)$] is preferentially followed by the Co fcc grains that grow on top, whereas the reversed Co stacking,

with peak at $L=1.1$, is less favored by a factor of around 2, as deduced from the intensities ratio.

However, the most relevant and new information contained in Fig. 2(b) is the drastic change in the Co film stacking distribution after depositing a 4 AL Gd overlayer; both fcc contributions disappear (only a small asymmetry is still observed at the majority fcc stacking position, $L=2.2$), whereas the hcp stacking remains almost unchanged. This observation, combined with the reduction in the in-plane Co peak intensity at $L=0.5$ observed in Fig. 1, suggests that the Co film is being partially amorphized and that, in addition, this disordering is preferentially affecting the Co crystals with fcc stacking. The higher resistance to disordering of hcp crystallites compared to fcc ones is consistent with the fact that hcp is the equilibrium structure of Co at temperatures below 695 K.[32] It should be pointed out that the results of Fig. 2(b) were carefully checked to be free of systematic errors as those related to small misalignments. Subsequent growths of Gd up to completing 15 AL produced just very tiny effects on the L scan: a 7% reduction in the height of the hcp peak at $L=1.65$ and a further reduction in the small fcc shoulder remaining at $L=2.2$, that could be simply related to absorption effects by the thickest Gd layer. This suggests that the main disordering took place during the first steps of Gd growth, leading to an intermediate mixed amorphous Co-Gd layer that passivates the amorphization process so that additional amounts of Gd are not able to complete the amorphization of the whole 15 AL Co film. This passivation effects are in good agreement with previous findings indicating that the amorphization of Co films by Gd overlayers is less pronounced than the opposite situation of Gd films amorphized by Co overlayers.[6]

Theoretical support to the experimentally observed preferential disordering of the less stable fcc Co grains, as compared to hcp ones, can be found in thermodynamic considerations based on the different surface energy of the hcp and fcc Co phases. Calculations based on the linear muffin-tins orbital method[33] indicate that the surface energy of the Co(111) fcc stacking, γ_{Co} (fcc)$=3.23$ J/m^2, is higher than that of the Co(001) hcp arrangement, γ_{Co} (hcp) $=2.74-3.18$ J/m^2. Surface energy is one of the parameters affecting the amorphization of Co/Gd multilayers, as studied in detail by Alonso *et al.*,[17] who have developed a phenomenological model to study the compositional range of amorphization in Co/Gd multilayers which is in good agreement with their experimental findings.[34] Their model includes interfacial contributions, dependent on the surface energies of the interfaces involved in a Gd/Co multilayer, that modify the Gibbs free energy of the unreacted system and affect the stability of the initial unmixed configuration.[17] According to it, and taking into account that $\gamma_{\mathrm{Co}}(\mathrm{fcc}) > \gamma_{\mathrm{Co}}(\mathrm{hcp})$, the estimated excess Gibbs free energy, and thus, the thermodynamical driving force for mixing, in a Gd/Co multilayer, are higher for the fcc case than for hcp Co grains: $\Delta G_{\mathrm{multilayer}}(\mathrm{fcc}) > \Delta G_{\mathrm{multilayer}}(\mathrm{hcp})$. Consequently, our experimental observations appear to be driven by thermodynamics.

The evidence of disordering provided by the out-of-plane scans can be used to explain the origin of the in-plane Co peak shift shown in Fig. 1. In fact, a closer look into the H values of the Co peak in Fig. 1 reveals interesting details. The 15 AL Co peak has a maximum at around $H=1.097$ rlu, as determined from Gaussian fitting with an error in the peak position determination smaller than 10^{-3} rlu, although the expected value for a completely relaxed Co film is 1.106 rlu, given by the ratio of the relaxed interatomic distances of Pt and Co: $a_{\mathrm{Pt}}/a_{\mathrm{Co}}=2.772$ Å/2.506 Å. This means that the as-grown Co film still has some residual strain, with an in-plane unit cell slightly expanded by about 0.009 rlu. However, after growth of the 4 AL Gd overlayer (see Fig. 1), the Co peak shifts up to 1.102 rlu, much closer to the expected relaxed value for Co. In fact, the change in peak shape is not exactly a shift, but a reduction in area and narrowing of the peak [from full width at half maximum (FWHM) = 0.025 to 0.023 rlu] affecting only its low H value side, whereas the high H value side remains unchanged. This asymmetric narrowing has as a consequence the shift of the peak maximum toward the relaxed position. The reduction in Co peak area is a clear indication of disordering induced by the Gd overlayer, and the asymmetry suggests that this partial amorphization is affecting preferentially the more strained Co grains, which correspond to the low H values side of the peak. In fact, this low H contribution is related to Co grains with a larger interatomic distance, where Gd atoms could diffuse better, mix and disorder more easily the Co network. The comparison with the out-of-plane scans suggests a link between these strained low H contributions to the in-plane Co peak and the fcc stacking of the out-of-plane (1.1 −1.1 L) scans, since both of them disappear after the 4 AL Gd overlayer growth. So the combined analysis of in-plane and out-of-plane measurements suggests that fcc Co grains, which are preferentially amorphized, have an in-plane unit cell slightly larger than hcp grains. This extra strain provides an additional contribution to their instability and to their tendency to amorphize.

Similar structural results have been obtained when studying the disordering of a 15 AL Co film grown at RT. In this case, growth oscillations are completely damped after three to four periods, meaning that the films is rougher than the LT one, and suggesting a higher disorder. In fact, this increased disorder is confirmed by the in-plane (H −H 0.5) radial scan after RT Co growth, which shows a Co peak at the same position than the one from the film grown at LT (see Fig. 1), but having a relative intensity with respect to the Pt (1 −1 0.5) peak reduced by a factor of 7. Furthermore, the FWHM in the azimuthal scans around the Co peak increased from 1.8° (LT) to 2.2° (RT), indicating a reduction in Co grain size. Again, as it happened for the LT Co film, the growth of Gd overlayers (which, in order to keep the same situation than in the LT case apart from the Co growth temperature, has been carried out after cooling down the film to 200 K) leads to a shift of the Co peak toward higher values in H (0.6% relative shift for 4 AL of Gd in this case) also associated to a decrease in peak area accompanied by an asymmetric narrowing of the width (from FWHM = 0.033 to 0.027 rlu). The result is that the Co peak after partial amorphization approaches the position corresponding to a more relaxed film than the starting one. This suggests that, as in the case of the LT Co film, the more strained grains are more susceptible to get disordered than the less strained ones.

The evolution of the out-of-plane stacking again shows a preferential disordering of the fcc grains, although in this

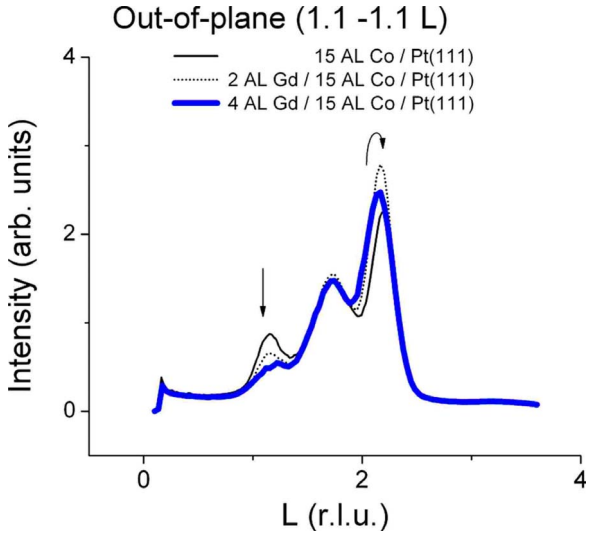

FIG. 3. (Color online) Experimental out-of-plane (1.1 −1.1 *L*) scans for the 15 AL Co/Pt(111) structure grown at RT (thin line), after depositing 2 AL Gd overlayer (dotted line) and after depositing 4 AL Gd (thick line).

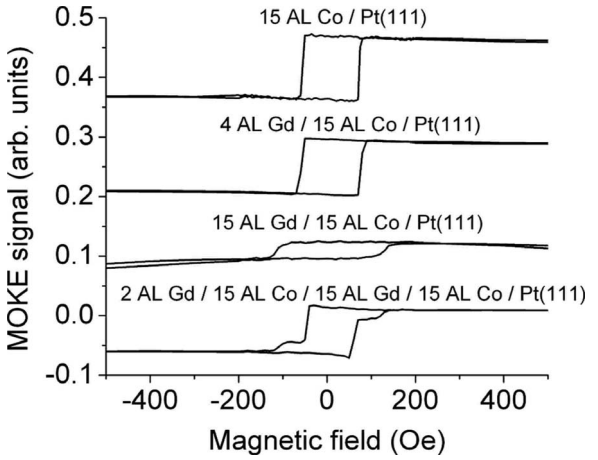

FIG. 4. MOKE loops acquired at different steps of a 2 AL Gd/15 AL Co/15 AL Gd/15 AL Co/Pt(111) LT growth. The loops have been vertically shifted for clarity.

case the situation is slightly more complex than in the LT Co film, as can be seen in the (1.1 −1.1 *L*) scans shown in Fig. 3. As expected from previous work,[26] the stacking distribution of the 15 AL Co film grown at RT (thin line of Fig. 3) has drastically changed as compared to the LT Co film of the same thickness [thin line of Fig. 2(b)]. Whereas the LT Co film was a mixture of fcc, hcp, and disorder, the RT Co film has a much lower hcp content (as indicated by the low intensity at $L=3.3$ and $L=0$) and the fcc and disordered stackings are clearly dominant, confirming previous results.[26] As it happened for the LT growth case, Co grains keeping the substrate fcc stacking sequence (peak at $L=2.2$) dominate with respect to their corresponding (111) twin (peak at $L=1.1$).

The results concerning the disordering of this RT 15 AL Co film are shown in Fig. 3 for two Gd overlayer thicknesses, 2 AL (dotted line), and 4 AL (thick line). The 2 AL growth, and the previous steps measured during growth but not shown, indicate a continuous trend to reduce the minority fcc stacking and to increase the majority one, suggesting that Co atoms are transferred from the minority to the majority stacking, whereas the intensity arising from disordered stacking planes remains basically unaltered. Additional growth of Gd, up to 4 AL, continue the reduction in the minority stacking and start to reduce also the majority one. A closer look into the peak at $L=2.2$ shows that the majority stacking peak is continuously shifting toward lower L values, meaning that the interplanar average distance is slightly increasing, most likely due to the distortions induced by the bigger Gd atoms entering the Co network.

These RT film results confirm that disordering is again selectively acting on the stacking, and again, minority fcc stacking is the most affected by disordering, as in the case of the LT film, where no traces of peak at $L=1.1$ were left, whereas a small shoulder was still present at $L=2.2$ [see Fig. 2(b)]. The results presented in Figs. 2(b) and 3 indicate that disordering is stacking dependent, acting preferentially on the minority fcc stacking, which is more strained than the majority one, as indicated by the positions of the diffracted peaks. The predominance of one of the two, in principle equivalent, fcc stackings and its larger resistance to disordering as compared to the minority one, is a consequence of a long-range interaction involving second-plane neighbors. This kind of interactions, favoring one of the two types of fcc stacking, reminds previous results in Ni/Pt epitaxial multilayers, where Ni grows preferentially following the Pt fcc substrate stacking, whereas Pt reverses its stacking when grown on top of Ni.[35] On the other hand, the observed stability of the disordered stacking in Fig. 3 against alloying with Gd suggests that this disordered sequence would be closer to a pure hcp, which was the more stable in the LT growth than to a pure fcc stacking.

To summarize this section, growth of Co/Gd structures results in appreciable disordering processes that affect preferentially the less stable fcc stackings. These processes may be rationalized with thermodynamical arguments which indicate that fcc stackings are more susceptible to disordering than hcp ones, and are accompanied by a reduction in the in-plane lattice unit cell of about 0.4%–0.6%, related to the relaxation of the Co film through disordering of strained fcc grains.

B. Magnetic characterization

The magnetic properties of these Co films, before and after disordering by Gd overlayers, have been studied by MOKE measurements, which are sensitive to Co (but, as already mentioned, not to Gd and Pt) magnetization, and also, by Pt RM-SXRD cycles sensitive to the Pt magnetism at the interface. As Pt RM-SXRD measurements are more time consuming, they have been acquired only at selected steps of the growth sequence. Figures 4 and 5 show the corresponding MOKE loops (vertically shifted for clarity), and RM-SXRD Pt cycles, respectively. First thing to point out is that the LT 15 AL Co film has a square shape loop, with a coercive field around 60 Oe, typical of a situation where the critical thickness for the out-of-plane/in-plane anisotropy

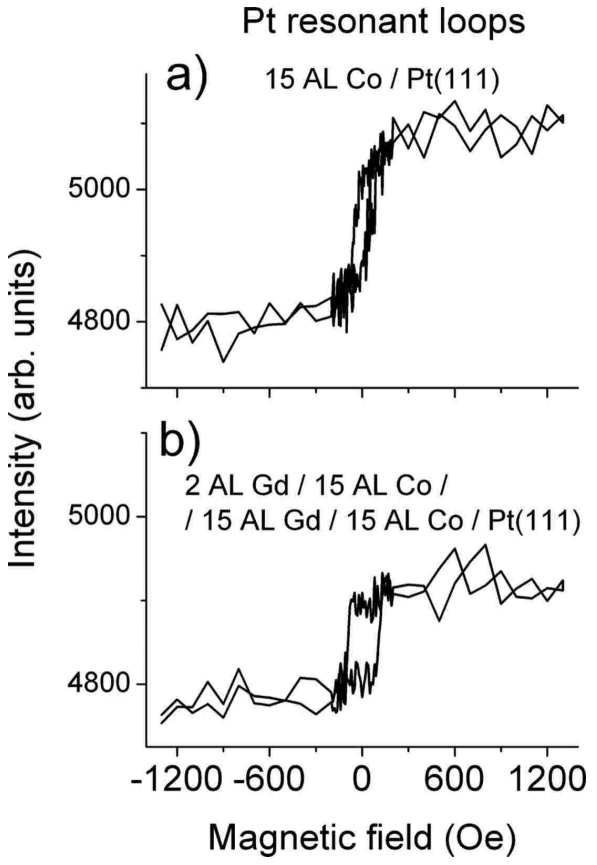

FIG. 5. Pt L_{III} resonant diffraction loops, measured at (1 −1 3.6), (a) after deposition of the first 15 AL Co layer, and (b) after growing a Gd/Co/Gd/Co/Pt(111) stacking at LT.

transition has been crossed and Co magnetization lies in the film plane. Second information is that deposition of the Gd overlayer produces changes in the magnetic loops since the first steps. The 4 AL Gd/15 AL Co/Pt(111) structure has a smaller MOKE intensity and a less square loop. This is compatible with a situation where some Gd is amorphizing the Co top atoms leading to a less marked in-plane anisotropy than the one corresponding to an epitaxial Co crystalline film. Further growth of Gd, up to 15 AL, significantly increases the coercive field up to 120 Oe, and reduces the MOKE signal even more. The reduction in MOKE intensity may be explained by the formation of an amorphous Co-Gd alloy on top of the Co film, leading to a decrease in density of Co atoms and also to a reduction in the Co magnetic moment.[36] The increase in coercive field can also be explained by the presence of an amorphous Co-Gd alloy layer since these alloys are usually magnetically harder than pure Co films. In fact, amorphous Co-Gd alloys have a coercive field that diverges at the compensation temperature,[37,38] that, for low Gd content, is below our measuring temperature of 200–220 K.[39] Increasing the Gd layer thickness should increase the effective Gd concentration of the amorphous Co-Gd layer, which is known to shift the compensation temperature to higher values[39] that approach the temperature of our measurements, causing an increase in the coercive field, as observed.

In order to study the magnetic coupling through the Gd overlayer, a second 15 AL Co film, with a 2 AL Gd overlayer, was grown on top of the 15 AL Gd layer. The corresponding cycle has a stepped behavior with increased MOKE signal, as it is shown in Fig. 4. The shape of this loop reveals that there are two uncoupled magnetic contributions, one that reverses at lower field, again 60 Oe, associated to the top Co film, and another that reverses at higher field, 120 Oe, related to the Co-Gd alloy and lower Co film.

The corresponding resonant magnetic Pt hysteresis loops at the Co/Pt (111) interface are shown in Fig. 5. As already mentioned, they have been measured at a fixed position in reciprocal space, (1 −1 3.6), where the resonant signal is maximum. As known, Pt is magnetically polarized due to the hybridization with the Co atoms deposited on top, leading to a Pt-Co interface where out-of-plane (i.e., perpendicular) anisotropy dominates. When Co thickness is above a certain threshold, usually few Co monolayers, magnetization becomes parallel to the sample plane. This means that the Pt magnetization is expected to follow the magnetic behavior of the Co atoms closer to the interface. In agreement with these expectations, the Pt loop corresponding to the first step of growth, 15 AL Co/Pt(111), has a coercive field similar to the corresponding Co one measured by MOKE [see first cycle of Fig. 4 and loop of Fig. 5(a)], 60 Oe. It is worth noting, however, that the shape of the two loops is slightly different. As already mentioned, the MOKE loop is square, indicating a well-defined in-plane anisotropy. On the other hand, the Pt loop is clearly less square, most likely reflecting the strong trend of the magnetization at the interface to align in a perpendicular configuration.

The Pt magnetization after growing the whole sequence has significantly changed, as can be seen in Fig. 5(b). Two effects are observed. First one is a strong increase in coercive field up to around 100 Oe. This confirms that the trend shown in the loops of Fig. 4, where the coercive field is continuously increasing with the Gd overlayer thickness, is affecting the whole Co layer down to the Pt interface, which reverses its magnetization at a much higher field than before depositing the Gd overlayer. Second, the height of the loop, usually quantified through the asymmetry ratio $R=(I^+ - I^-)/(I^+ + I^-)$, where I^+ (I^-) is the diffracted intensity for positive (negative) saturation, reduces significantly from around 3.0% down to 1.4%. The reason for this reduction is not clear at present. It could happen that the disordering affecting the fcc stacking is proceeding down to the Co-Pt interface, leading to a reduction in the effective magnetic moment of the Co atoms in contact with the Pt and, consequently, also to a reduction in the Pt magnetization and the jump in the loop. Some indications in this sense can be obtained when estimating the thickness of the fcc Co regions before disordering. From the FWHM of the majority fcc contribution to the L scan of Fig. 2(b) before Gd growth (FWHM=0.28 rlu, obtained after deconvolution of the scan with three Lorentzian components), an estimated thickness of 24 Å can be given for the fcc regions. This means that the complete amorphization by Gd of these grains could approach the Co-Pt interface since the Co film thickness is around 31 Å thick, and, hence, affect the Pt magnetization and the height of the Pt loop, as observed in Fig. 5(b), although additional data are needed to elucidate this point.

Finally, it should be noted that for the case of 15 AL Co film grown at RT, deposition of 2–4 AL thick Gd overlayers

makes the MOKE loops (not shown) less squared, meaning that the in-plane magnetic anisotropy of the starting Co film is less well defined, whereas the corresponding resonant magnetic Pt loop (not shown) mimics the Co behavior. This confirms that again, as for the case of LT films, the changes induced in the magnetic behavior of the system by depositing Gd overlayers affect the whole Co layer down to the Co/Pt interface.

IV. CONCLUSIONS

In summary, disordering of 15 AL thick Co films by Gd overlayers has been investigated with surface x-ray diffraction. The stacking structure of the Co films (mixture of hcp, fcc, and disordered) has varied depending on the substrate temperature during growth. It has been found that cubic fcc stacking is preferentially disordered as compared to hcp one. This effect has been discussed in terms of thermodynamic considerations. Moreover, the part of the Co film with the same stacking than that of the Pt substrate disorders less than that with the reversed (twin) stacking. Accompanying these structural changes, a small increase in the Co interatomic distance in the film plane, around 0.5%, was observed, indicative of strain relief. This allowed to associate the strained Co atoms with the preferentially disordered Co fcc grains. The corresponding magnetic hysteresis loops showed that the Gd overlayers modify significantly the magnetism of the Co film. The increase in coercive field and reduction in loop amplitude observed for thick enough Gd overlayers are compatible with formation of a disordered Co-Gd alloy having reduced Co magnetic moment. This changes in the magnetic behavior affect the whole Co film down to the Pt interface, as evidenced by Pt resonant magnetic scattering loops. All these results illustrate how surface x-ray diffraction can be used to elucidate the structural details of disordering processes happening in thin films of binary systems containing mixtures of different phases.

ACKNOWLEDGMENTS

Work was supported by the FIS2005–07392 and FIS2008–06249 grants. C.Q. acknowledges support from the Spanish Government and European Social Fund under the "Ramón y Cajal" program. H. Isérn, V. A. Solé, L. Petit, T. Dufrane, and H. Gonzalez are acknowledged for technical support. R. Morales, J. I. Martín, and J. M. Alameda are acknowledged for scientific discussions.

*Corresponding author. carquir@string1.ciencias.uniovi.es

†Present address: Université de Bourgogne–Institut Carnot de Bourgogne, 9 avenue Savary, 21078 Dijon, France.

[1] P. Hansen, in *Handbook of Magnetic Materials*, edited by K. H. J. Buschow (Elsevier, Amsterdam, 1991), Vol. 6, p. 289.

[2] S. Demirtas, M. R. Hossu, R. E. Camley, H. C. Mireles, and A. R. Koymen, Phys. Rev. B **72**, 184433 (2005).

[3] P. Chaudhari, J. J. Cuomo, and R. J. Gambino, Appl. Phys. Lett. **22**, 337 (1973).

[4] H. Fu, M. Mansuripur, and P. Meystre, Phys. Rev. Lett. **66**, 1086 (1991).

[5] D. Raasch and H. Wierenga, J. Magn. Magn. Mater. **168**, 336 (1997).

[6] T. C. Hufnagel, S. Brennan, A. P. Payne, and B. M. Clemens, J. Mater. Res. **7**, 1976 (1992).

[7] G. A. Bertero, T. C. Hufnagel, B. M. Clemens, and R. Sinclair, J. Mater. Res. **8**, 771 (1993).

[8] B. M. Clemens and T. C. Hufnagel, J. Alloys Compd. **194**, 221 (1993).

[9] J. B. Pelka, W. Paszkowicz, P. Dluzewsk, E. Dynowska, A. Wawro, L. T. Baczewski, M. Kozlowski, A. Wisniewski, O. Seeck, S. Messoloras, and H. Gamari-Seale, J. Phys. D **34**, A208 (2001).

[10] J. B. Pelka, W. Paszkowicz, A. Wawro, L. T. Baczewski, and O. Seeck, J. Alloys Compd. **328**, 253 (2001).

[11] J. P. Andrés, J. L. Sacedón, J. Colino, and J. M. Riveiro, J. Appl. Phys. **87**, 2483 (2000).

[12] J. Colino, J. P. Andrés, J. M. Riveiro, J. L. Martínez, C. Prieto, and J. L. Sacedón, Phys. Rev. B **60**, 6678 (1999).

[13] J. P. Andrés, L. Chico, J. Colino, and J. M. Riveiro, Phys. Rev. B **66**, 094424 (2002).

[14] J. A. González, J. P. Andrés, M. A. Arranz, M. A. López de la Torre, and J. M. Riveiro, J. Phys.: Condens. Matter **14**, 5061 (2002).

[15] J. A. González, J. P. Andrés, M. A. López de la Torre, and J. M. Riveiro, J. Appl. Phys. **93**, 7247 (2003).

[16] R. Morales, J. I. Martín, and J. M. Alameda, Phys. Rev. B **70**, 174440 (2004).

[17] J. A. Alonso, R. Hojvat de Tendler, D. A. Barbiric, and J. M. Riveiro, J. Phys.: Condens. Matter **14**, 8913 (2002).

[18] K. H. J. Buschow, J. Appl. Phys. **53**, 7713 (1982).

[19] N. H. Duc and D. Givord, J. Magn. Magn. Mater. **157-158**, 169 (1996).

[20] A. Heesemann, V. Zöllmer, K. Rätzke, and F. Faupel, Phys. Rev. Lett. **84**, 1467 (2000).

[21] F. Machizaud, K. Ounadjela, and G. Suran, Phys. Rev. B **40**, 587 (1989).

[22] C. Quirós, J. I. Martín, L. Zárate, M. Vélez, and J. M. Alameda, Phys. Rev. B **71**, 024423 (2005).

[23] F. Stein and G. Dietz, J. Magn. Magn. Mater. **117**, 45 (1992).

[24] P. Vojtanik, M. Boskovicova, E. Kisdi-Koszo, and A. Lovas, J. Magn. Magn. Mater. **41**, 385 (1984).

[25] O. Robach, C. Quiros, P. Steadman, K. F. Peters, E. Lundgren, J. Álvarez, H. Isern, and S. Ferrer, Phys. Rev. B **65**, 054423 (2002); **71**, 099903(E) (2005).

[26] C. Quirós, S. M. Valvidares, O. Robach, and S. Ferrer, J. Phys.: Condens. Matter **17**, 5551 (2005).

[27] S. Ferrer and F. Comin, Rev. Sci. Instrum. **66**, 1674 (1995).

[28] F. de Bergevin, M. Brunel, R. M. Galéra, C. Vettier, E. Elkaïm, M. Bessière, and S. Lefèbvre, Phys. Rev. B **46**, 10772 (1992).

[29] S. Ferrer, P. Fajardo, F. de Bergevin, J. Alvarez, X. Torrelles, H. A. van der Vegt, and V. H. Etgens, Phys. Rev. Lett. **77**, 747

(1996).
[30] E. Lundgren, B. Stanka, G. Leonardelli, M. Schmid, and P. Varga, Phys. Rev. Lett. **82**, 5068 (1999).
[31] A. Guinier, *X-Ray Diffraction in Crystals, Imperfect Crystals and Amorphous Bodies* (Dover, New York, 1994).
[32] P. Tolédano, G. Krexner, M. Prem, H.-P. Weber, and V. P. Dmitriev, Phys. Rev. B **64**, 144104 (2001).
[33] H. L. Skriver and N. M. Rosengaard, Phys. Rev. B **46**, 7157 (1992).
[34] J. A. González, J. P. Andrés, M. A. López de la Torre, and J. M. Riveiro, J. Magn. Magn. Mater. **242-245**, 547 (2002).
[35] O. Robach, C. Quirós, H. Isérn, P. Steadman, K. F. Peters, and S. Ferrer, Phys. Rev. B **67**, 220405(R) (2003).
[36] R. C. Taylor and A. Gangulee, J. Appl. Phys. **47**, 4666 (1976).
[37] Y. Togami, IEEE Trans. Magn. **18**, 1233 (1982).
[38] M. H. Kryder, H.-P. Shieh, and D. K. Hairston, IEEE Trans. Magn. **23**, 165 (1987).
[39] P. Hansen, C. Clausen, G. Much, M. Rosenkranz, and K. Witter, J. Appl. Phys. **66**, 756 (1989).